HAL
open science

Numerical scheme for multilayer shallow-water model in the low-Froude number regime

Martin Parisot, Jean-Paul Vila

To cite this version:

Martin Parisot, Jean-Paul Vila. Numerical scheme for multilayer shallow-water model in the low-Froude number regime. Comptes rendus de l'Académie des sciences. Série I, Mathématique, 2014, 352, pp.953 - 957. 10.1016/j.crma.2014.09.020 . hal-01079843

HAL Id: hal-01079843

https://inria.hal.science/hal-01079843v1

Submitted on 3 Nov 2014

HAL is a multi-disciplinary open access archive for the deposit and dissemination of scientific research documents, whether they are published or not. The documents may come from teaching and research institutions in France or abroad, or from public or private research centers.

L'archive ouverte pluridisciplinaire **HAL**, est destinée au dépôt et à la diffusion de documents scientifiques de niveau recherche, publiés ou non, émanant des établissements d'enseignement et de recherche français ou étrangers, des laboratoires publics ou privés.

Numerical scheme for multilayer shallow-water model in the low-Froude number regime ⋆

M. PARISOT [a] J.P. VILA [b],

[a] *Institut de Mathmatiques de Toulouse, UMR CNRS 5219, UPS IMT, F-31062 Toulouse Cedex 9, France*
[b] *Institut de Mathmatiques de Toulouse, UMR CNRS 5219, INSA, F-31077 Toulouse, France*

Received *****; accepted after revision +++++

Presented by

Abstract

The aim of this note is to present a multi-dimensional numerical scheme approximating the solutions of the multilayer shallow water model in the low Froude number regime. The proposed strategy is based on a regularized model where the advection velocity is modified with a pressure gradient in both mass and momentum equations. The numerical solution satisfy the dissipation of energy, which act for mathematical entropy, and the main physical properties required for simulations within oceanic flows.

Résumé

Schéma numérique pour les modèles de Saint-Venant multi-couche à faible nombre de Froude. Le but de cette note est de présenter un schéma numérique multi-dimensionnel rapprochant les solutions du modèle de Saint-Venant multi-couche en régime de faible nombre de Froude. La stratégie proposée est basée sur un modèle régularisé où la vitesse de transport est modifié par un gradient de pression dans les équations de la masse et de la quantité de mouvement. La solution numérique satisfait la dissipation d'énergie, jouant le rôle de l'entropie du point de vue mathématique, et les principales propriétés physiques nécessaires aux simulations dans le cadre des écoulements océanique.

1. Introduction

The current note is devoted to the numerical resolution of the multilayer shallow water model. Let us consider a set of L immiscible, homogeneous, inviscid and incompressible superposed fluids with free surface and without surface tension. The pressure is assumed to be hydrostatic and constant at the free

⋆. This work was supported by the French Naval Hydrographic and Oceanographic Service.
Email addresses: `parisot@insa-toulouse.fr` (M. PARISOT), `vila@insa-toulouse.fr` (J.P. VILA).

surface. In addition, we supposed that the vertical acceleration is small enough to make the flow satisfies the shallow water assumption. The ith layer of fluids has a constant density ρ_i, a thickness $h_i(t,x)$ and a depth-averaged horizontal velocity $v_i(t,x)$ with $t \geq 0$ design the time variable and $x = (x_1, x_2) \in \mathbb{R}^2$ the horizontal position. The governing equations are given by the multilayer shallow water equations, i.e.

$$(SW) \begin{cases} \partial_t h_i \quad + \nabla_x \cdot (h_i v_i) & = 0, \\ \partial_t (h_i v_i) + \nabla_x \cdot (h_i v_i \otimes v_i) + \dfrac{h_i}{\rho_i} \nabla_x p_i & = 0, \end{cases} \tag{1}$$

with g is the gravitational acceleration and the pressure is given by the hydrostatic relation, i.e. $p_i = g \sum_{j=1}^{L} \rho_{\min(i,j)} h_j$ with the layer numbered downwards from the free surface. The multi-layer shallow water model (1) could be obtained from Euler equations by vertical averaging across the layer depth, see [2]. Previous studies present criterium of well-posedness for the multilayer shallow water model (1), see [7,9]. In particular, the layers should be organized with the heaviest at bottom to the lightest at the top, i.e. $\rho_1 < \rho_2 < \cdots < \rho_{L-1} < \rho_L$. In addition, the vertical variation of velocity should be small enough in comparison to the layer thickness, more precisely a required condition for the hyperbolicity of (1) reads

$$\frac{\|v_{i+1} - v_i\|^2}{g(h_{i+1} + h_i)} < 1 - \frac{\rho_i}{\rho_{i+1}}. \tag{2}$$

The main features of the multilayer shallow water model are its mathematical structure, more precisely hyperbolic for reasonable regime, and the underlying conservative laws. More precisely, the multilayer shallow water model preserves the water volume of each layer (first equation of (1)), the momentum of the column of water

$$\partial_t \sum_{i=1}^{L} (\rho_i h_i v_i) + \nabla_x \cdot \sum_{i=1}^{L} (\rho_i h_i v_i \otimes v_i) + \nabla_x \mathcal{E} = 0 \tag{3}$$

and the total energy $E = \mathcal{E} + \mathcal{K}$ (for smooth solutions)

$$\partial_t E + \nabla_x \cdot \sum_{i=1}^{L} ((2\mathcal{E}_i + \mathcal{K}_i) v_i) = 0 \tag{4}$$

where the potential energy is defined by $\mathcal{E} = \sum_{i=1}^{L} \mathcal{E}_i$ with $\mathcal{E}_i = \frac{1}{2} h_i p_i$ and the kinetic energy is defined by $\mathcal{K} = \sum_{i=1}^{L} \mathcal{K}_i$ with $\mathcal{K}_i = \frac{1}{2} \rho_i h_i \|v_i\|^2$.

In the current work, we are interesting into application of the multilayer shallow water model to describe ocean environment characterized by a weakly stratified density, i.e. $0 < 1 - \frac{\rho_i}{\rho_{i+1}} \ll 1$, see [8]. The multilayer shallow water model could be used to describe weakly stratified flows assuming that the Froude number is small enough in a suitable referencial such that the required condition (2) holds. Classical numerical schemes used to approximate shallow water models, like Riemann solvers, require the estimation, or at least an upper bound, of the eigenvalues. In [5] and [1], the authors present a numerical strategy based on the estimation of the eigenvalues realized in [11]. This estimation is valable for weakly stratified density and in the two layer case. It is hardly adaptable to an arbitrary number of layers and for all stratifications. In [3] and [4], the authors present a strategy to adapt the resolution of the mono-layer case, currently well-known, to the multi-layer case. However, these solvers are well-known to be too much dissipative in the low-Froude number regime, and lead to restrictive CFL condition in the context of oceanic flow.

To overcome these drawbacks, we adapt the numerical scheme presented in [12] for multiphasic Euler equations in low-Mach number regime. This strategy does not require estimation of eigenvalues and is able to recover low-Mach number flows. The multilayer shallow water model introduces new difficulties in comparison to the multiphasic Euler equations. More precisely, the number of unknowns is larger since the velocities of each layer are not the same and the pressure term is not conservative in the multilayer shallow water model.

2. Regularized model

As it is shown in [6], the low-Froude number regime, by analogy with the low-Mach number regime, require the centered discretization of the pressure term. However, this discretization introduce numerical source term of the discrete energy which leads to unstable solution. To overcome this difficulty, the key point is to modify the convective discharge in both mass conservation and momentum balance such that the regularized model yields

$$(SW_\varepsilon)\begin{cases}\partial_t h_i^\varepsilon \quad + \nabla_x \cdot q_i^\varepsilon = 0,\\ \partial_t\left(h_i^\varepsilon v_i^\varepsilon\right) + \nabla_x \cdot \left(q_i^\varepsilon \otimes v_i^\varepsilon\right) + \dfrac{h_i^\varepsilon}{\rho_i}\nabla_x p_i^\varepsilon = 0.\end{cases} \tag{5}$$

The regularized model (5) still satisfies the conservation of the column of water (3), and instead of conservation law (4), it satisfies the following total energy balance

$$\partial_t E^\varepsilon + \nabla_x \cdot \sum_{i=1}^{L}\left(\left(2\mathcal{E}_i^\varepsilon + \mathcal{K}_i^\varepsilon\right)\frac{q_i^\varepsilon}{h_i^\varepsilon}\right) = \sum_{i=1}^{L}\left(q_i^\varepsilon - h_i^\varepsilon v_i^\varepsilon\right)\cdot\nabla_x p_i^\varepsilon. \tag{6}$$

Choosing the effective discharge q_i^ε such that the right-hand-side is negative, equation (6) leads to dissipation of the total energy which acts for mathematical entropy of the system. More precisely, we set $q_i^\varepsilon = h_i^\varepsilon v_i^\varepsilon - \varepsilon\gamma\frac{H^\varepsilon}{\rho_i}\nabla_x\pi_i^\varepsilon$ with the regularizing pressure π_i^ε function of $\left(h_j^\varepsilon\right)_{j\in[\![1,L]\!]}$, the total water elevation $H^\varepsilon = \sum_{i=1}^{L} h_i^\varepsilon$, a dimensionless parameter $\gamma > 0$ defined further and a time scale $\varepsilon > 0$. Assuming that the regularizing function π_i^ε is smooth enough, the shallow water model (1) is formally recovered at the limit ε goes to zero. A trivial choice of the regularizing pressure is $\pi_i^\varepsilon := p_i^\varepsilon$ and leads to a notable estimation of the variation of the pressure, i.e.

$$\int_0^T\int_{\mathbb{R}^2}\varepsilon\gamma H^\varepsilon\sum_{i=1}^{L}\frac{\|\nabla_x p_i^\varepsilon\|^2}{\rho_i}\,\mathrm{d}x\,\mathrm{d}t \le \int_{\mathbb{R}^2} E\left(0,x\right)\,\mathrm{d}x.$$

We discuss further about a more effective choice in term of computational efficiency.

Let consider a tessellation of $\mathbb{R}^2$ denote $\mathbb{T}$. For any polygon $k \in \mathbb{T}$, we design by $|k|$ its area and by $\mathbb{F}_k$ its set of edges. In addition, for any edge $f \in \mathbb{F}_k$, we design by $|f|$ its lengh and by $k_f \in \mathbb{T}$ the neighbor of k such that $k \cap k_f = f$. Similarly, we introduce a time discretization with Δt the time step such that $t^{n+1} = t^n + \Delta t$. The numerical strategy presented is this work is based on a cell-centered finite volume methods, i.e. the numerical unknowns are in each polygon $k \in \mathbb{T}$ and each layer $1 \le i \le L$ the averaged-value of the layer thickness $h_{i,k}^n$ and of the horizontal velocity $v_{i,k}^n$ where the superscript n is relative to the discrete time t^n.

The mass conservation of (5) could be compared to an advection-diffusion equation, which is classically discretized using an implicit time scheme with an upwind scheme decentered with respect to the velocity $v_{i,f}^n$ for the advection part and a centered scheme for the diffusion part. Then, the momentum balanced of (5) could be estimated explicitly. The numerical scheme reads

$$\begin{aligned}&\frac{h_{i,k}^{n+1} - h_{i,k}^n}{\Delta t} + \frac{1}{|k|}\sum_{f\in\mathbb{F}_k}\left(\left(q_{i,f}^{n+1}\cdot n_f^k\right)^{out} - \left(q_{i,f}^{n+1}\cdot n_f^k\right)^{in}\right)|f| = 0\\ &\frac{h_{i,k}^{n+1}v_{i,k}^{n+1} - h_{i,k}^n v_{i,k}^n}{\Delta t} + \frac{1}{|k|}\sum_{f\in\mathbb{F}_k}\left(v_{i,k}^n\left(q_{i,f}^{n+1}\cdot n_f^k\right)^{out} - v_{i,k_f}^n\left(q_{i,f}^{n+1}\cdot n_f^k\right)^{in}\right)|f| = -\frac{1}{|k|}\frac{h_{i,k}^{n+1}}{\rho_i}\sum_{f\in\mathbb{F}_k}p_{i,f}^{n+1}|f|\end{aligned} \tag{7}$$

with the discrete effective discharge outgoing and incoming the volume k through the face f such as

$$\left(q_{i,f}^{n+1}\cdot n_f^k\right)^{out} := h_{i,k}^{n+1}\left(v_{i,f}\cdot n_f^k\right)^+ + 2\gamma_f\frac{\varepsilon}{\Delta x_f}\frac{H_f^n}{\rho_i}\left(\delta\pi_{i,f}^{n+1}\cdot n_f^k\right)^- =: \left(q_{i,f}^{n+1}\cdot n_f^{k_f}\right)^{in}$$

and the positive and negative part functions, $2\phi^{\pm} = |\phi| \pm \phi \geq 0$. The following notations at the faces are used: $2\phi_f = \phi_k + \phi_{k_f}$ and $2\delta\phi_f = \left(\phi_{k_f} - \phi_k\right) n_f^k$ so that $\phi_k = \phi_f - \delta\phi_f \cdot n_f^k$ with n_f^k is the unit normal vector to the face f outward the control volume k. The characteristic length is defined by $|\partial k|\,\Delta x_k = |k|$ with $|\partial k| = \sum_{f\in\mathbb{F}_k}|f|$. In addition, the extremum values are defined by

$$\phi_{\max}^n = \max_{k\in\mathbb{T}}\max_{i\in[\![1,L]\!]}\left(\phi_{i,k}^n\right), \qquad \phi_{\min}^n = \min_{k\in\mathbb{T}}\min_{i\in[\![1,L]\!]}\left(\phi_{i,k}^n\right) \qquad \text{and} \qquad \delta\phi_{\max}^n = \max_{f\in\mathbb{F}}\max_{i\in[\![1,L]\!]}\left(\left\|\delta\phi_{i,f}^n\right\|\right).$$

From now on we set the time scale $\varepsilon := \Delta t$.

The main result of this note is the following stability result:

Proposition 1 *Assume that there exists a density $\overline{\rho} > 0$ such that the regularizing pressure $\pi_{i,k}^{n+1}$ satisfy*

$$\sum_{i=1}^{L}\frac{\delta\pi_{i,f}^{n+1}\cdot\delta p_{i,f}^{n+1}}{\rho_i} \geq \overline{\rho}\left(g\|\delta\mathbf{h}_f^{n+1}\|\right)^2 \quad \textit{with} \quad \delta\mathbf{h}_f^{n+1} = \left(\frac{h_{1,k_f}^{n+1}-h_{1,k}^{n+1}}{2},\ldots,\frac{h_{L,k_f}^{n+1}-h_{L,k}^{n+1}}{2}\right)^{\top}. \tag{8}$$

Then, defining the diffusion parameter by

$$\begin{aligned}\gamma_f = \frac{1}{2}\left(\frac{\widetilde{H}_f^{n+1}}{H_f^n} + \frac{\widetilde{V}_f^n\Delta x_f}{gH_f^n\Delta t}\right) \qquad &\textit{with} \qquad \widetilde{H}_f^{n+1} = \frac{\Delta x_f}{2}\sum_{i=1}^{L}\left(\left(\frac{h_{i,k}^{n+1}}{\Delta x_k} + \frac{h_{i,k_f}^{n+1}}{\Delta x_{k_f}}\right)\sum_{j=1}^{L}\frac{\rho_{\min(i,j)}}{\overline{\rho}}\right)\\ &\textit{and} \qquad \widetilde{V}_f^n = \sum_{i=1}^{L}\frac{\rho_{\min(i,j)}}{\overline{\rho}}\max\left(\left|v_{i,k}^n\cdot n_f^k\right|,\left|v_{i,k_f}^n\cdot n_f^k\right|\right)\end{aligned} \tag{9}$$

and under the following CFL condition $\left(v_{\max}^n + \alpha\sqrt{\frac{\delta\pi_{\max}^{n+1}}{\rho_1}}\right)\frac{\Delta t}{\Delta x_{\min}} \leq \beta$ with

$$\alpha = \frac{L}{2}\sqrt{\frac{\rho_L}{\overline{\rho}}\left(1+\frac{\Delta x_{\max}}{\Delta x_{\min}}\right)} \qquad \textit{and} \qquad \beta = \frac{h_{\min}^{n+1}}{2\left(h_{\max}^{n+1} + L\frac{\rho_L}{\rho_1}\frac{\delta\pi_{\max}^{n+1}}{g\overline{\rho}}\right)},$$

the numerical strategy keep the layer thickness non-negative, satisfy the steady state of the lake at rest $(h_i, u_i) = (Cst, 0)$ and satisfies the dissipation of the discrete total energy $E_k^n = \sum_{i=1}^{L}\left(\mathcal{E}_{i,k}^n + \mathcal{K}_{i,k}^n\right)$

$$E_k^{n+1} - E_k^n + \frac{\Delta t}{|k|}\sum_{f\in\mathbb{F}_k}\sum_{i=1}^{L}\left(G_{\mathcal{K},i,f}^{n+1}\cdot n_f^k + G_{\mathcal{E},i,f}^{n+1}\cdot n_f^k + \frac{\Delta t}{2\rho_i}\left(\frac{h_{i,k_f}^{n+1}}{\Delta x_{k_f}} - \frac{h_{i,k}^{n+1}}{\Delta x_k}\right)\left\|\delta p_{i,f}^{n+1}\right\|^2\right)|f| \leq 0$$

with the discrete potential energy $\mathcal{E}_{i,k}^n = \frac{1}{2}h_{i,k}^n p_{i,k}^n$, the discrete kinetic energy $\mathcal{K}_{i,k}^n = \frac{1}{2}\rho_i h_{i,k}^n\|v_{i,k}^n\|^2$, the discrete flux of potential energy $G_{\mathcal{E},i,f}^{n+1}$ and the discrete flux of kinetic energy $G_{\mathcal{K},i,f}^{n+1}$ respectively

$$\begin{aligned}&G_{\mathcal{E},i,f}^{n+1} = p_{i,f}^{n+1}q_{i,f}^{n+1}\cdot n_f^k - \delta h_{i,f}^{n+1}\cdot\delta p_{i,f}^{n+1}v_{i,f}^{n+1} - h_{i,f}^{n+1}\delta p_{i,f}^{n+1}\cdot n_f^k\frac{v_{i,k_f}^n - v_{i,k}^n}{2}\\ \textit{and} \qquad &G_{\mathcal{K},i,f}^{n+1} = \frac{1}{2}\rho_i\|v_{i,k}^n\|^2\left(q_{i,f}^{n+1}\cdot n_f^k\right)^{out} - \frac{1}{2}\rho_i\|v_{i,k_f}^n\|^2\left(q_{i,f}^{n+1}\cdot n_f^k\right)^{in}.\end{aligned}$$

In addition, the discrete water volume of each layer and the discrete momentum of the column of water are preserved (discrete version of (3)).

Note that the CFL condition of Proposition (1) is not optimal. However, in ocean environment, the water level is enough regular to make the celerity of the variation of pressure $\sqrt{\frac{g\delta\pi_{\max}}{\overline{\rho}}}$ small. In addition,

the velocity $v_{\max}$ is small and make together the CFL condition of Proposition (1) not restrictive, on the contrary of the CFL of a Riemann scheme limited by the gravity wave $\sqrt{gh_{\max}}$ large in this context.

The current version of the numerical scheme satisfies the steady state of the lake at rest without topography or other source terms. In a further work [10], we present an extension of the scheme satisfying the conservation of general steady state at rest and an adaptation to the geostrophic quasi-steady state.

On the pratical point of view, the layer thickness equation is non-linear through the diffusion parameter γ_f. We use a quasi-Newton fixed point estimating the diffusion parameter γ_f with the layer thickness of the previous fixed point iteration. The resulting linear system corresponds to a M-matrix (linear advection-diffusion operator) easily solvable using classical numerical tools. However, for oceanic simulations, the number of layers L could be large and the system become expensive to solved since the layer thickness equations are a priori coupled through the regularizing function π_i^ε. The computational efficiency of the strategy could be notably improved using a scheme estimating independently the layer thickness. The simple choice $\pi_i^\varepsilon := g\rho_i h_i^\varepsilon$ satisfy the hypothesis (8) of the proposition 1. In this way, the numerical scheme presents the advantage of the uncoupled Riemann strategy [3] while preserving the discrete momentum of the column of water conservation law and the entropy dissipation. Eventually, the numerical strategy presented does not require hypothesis on the flow regime as long as the flow is well-stratified, i.e. $\rho_1 < \cdots < \rho_L$. More precisely, it could be used as well for strongly stratified density with larger Froude number.

3. Numerical results

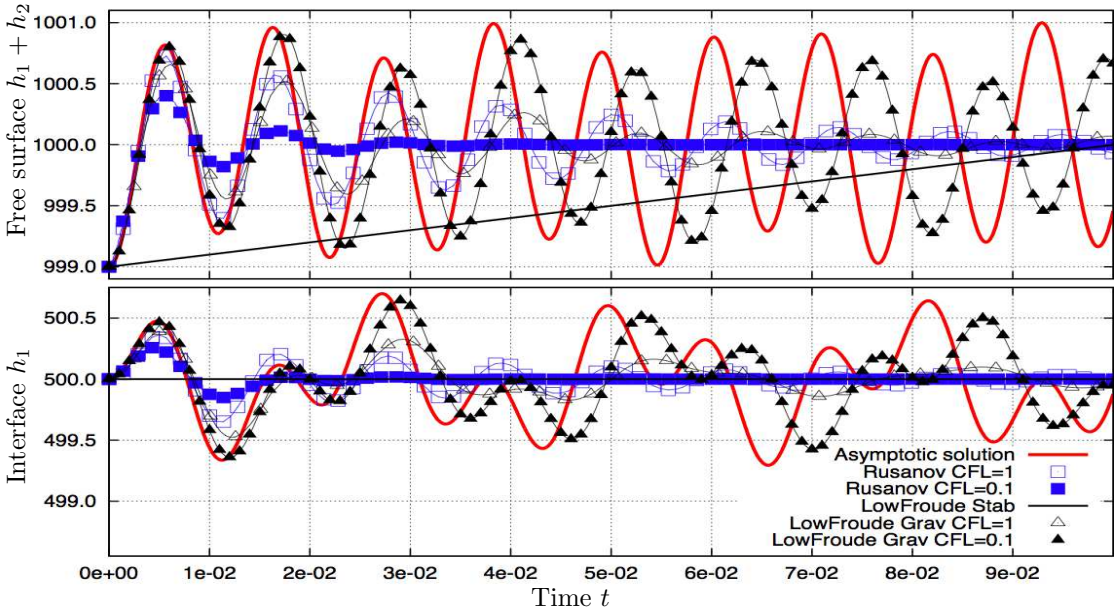

Figure 1. Interface elevations in function of time.

In this section we compare the numerical solution obtained using (7) to the linear solution in a low-Froude number regime in one dimension framework. The following numerical results are estimated using a coarse grid with 10 points by period, i.e. $|k| = \Delta x = 10^{-1}$. We consider the following initial condition in the whole 1D space

$$h_1 = 500 - \cos(2\pi x), \qquad h_2 = 500, \qquad v_1 = v_2 = 0, \qquad \frac{\rho_2}{\rho_1} = \frac{1}{2}.$$

In Figure 1, we plot the interface elevations at $x = 0$ as a function of time. The reference solution (red line "Asymptotic solution") is obtained assuming the solution is regular enough and neglecting the term in order to the square of the Froude number. The numerical solution "Rusanov" (blue line with square) are obtained using a Rusanov solver. For the best CFL conditon (empty square called "Rusanov CFL=1"), the Rusanov scheme is not able to recover the large frequences. The second simulation is obtained with a time step ten times smaller (fill square called "Rusanov CFL=0.1") and leads to more dissipative results. Using Riemann solver, the smaller the time step is, the more dissipative the resolution is. The numerical strategy (7) used with the diffusion parameter γ_f given by (9), is denoted "LowFroude" in Figure 1 (black line). The first simulation is obtained using the larger time step satisfying the CFL condition of Proposition 1 (black line without triangle called "LowFroude Stab"). The time step is too large to approach the gravity waves and the solution only recover the main term of the solution, i.e. the averaged value of the layer thickness. The second simulation (black line with empty triangle called "LowFroude Grav CFL=1") is obtained setting the time step to in the same order than the time step with a Riemann solver scheme. More precisely, we set $\Delta t = \frac{\Delta x}{\sqrt{gH^\star}}$ with the characteristic layer thickness $H^\star = 1000$. The numerical energy dissipation is similar to the case with the Riemann solver "Rusanov CFL=1", however the large frequences are recover. Finally, the last simulation is obtained using a fine time discretization, i.e. $\Delta t = 10^{-1}\frac{\Delta x}{\sqrt{gH^\star}}$ (black line with fill triangle "LowFroude Grav CFL=0.1") and leads to a better conservation of the system energy. Using the numerical scheme (7), the smaller the time step is, the less dissipative the resolution is.

References

[1] R. Abgrall and S. Karni. Two-layer shallow water system: a relaxation approach. SIAM J. Sci. Comput., 31:16031627, 2009.

[2] E. Audusse. A multilayer Saint-Venant model: derivation and numerical validation. Discrete Contin. Dyn. Syst. Ser. B, 5:189214, 2005.

[3] F. Bouchut and T. Morales de Luna. An entropy satisfying scheme for two-layer shallow water equations with uncoupled treatment. ESAIM Math. Model. Numer. Anal., 42:683698, 2008.

[4] F. Bouchut, V. Zeitlin, A robust well-balanced scheme for multi-layer shallow water equations, Discrete and Continuous Dynamical Systems - Series B, 13, 739-758, 2010.

[5] M. Castro, J. Macias and C. Pares, A Q-scheme for a class of systems of coupled conservation laws with source term, application to a two-layer 1-D shallow water system, M2AN Math. Model. Numer. Anal. 35, 107-127, 2001.

[6] S. Dellacherie. Analysis of Godunov type schemes applied to the compressible euler system at low mach number. J. Computational Phys., 229:9781016, 2010.

[7] V. Duchêne. Asymptotic shallow water models for internal waves in a two-uid system with a free surface. SIAM J. Math. Anal., 42:22292260, 2010.

[8] J. Gula, V. Zeitlin, F. Bouchut, Instabilities of buoyancy driven coastal currents and their nonlinear evolution in the two-layer rotating shallow water model. Part II. Active lower layer, J. Fluid Mech. 665, 209-237, 2010.

[9] R. Monjarret. Local well-posedness of the multi-layer shallow water model with free surface. To appear.

[10] M. Parisot and J.P. Vila. Centered-Potential Regularization of Advection Upstream Splitting Method: application to the multilayer shallow water model in the low-Froude number regime. to appear.

[11] R.R. Long, Long waves in a two-fluid system, J. Met., 13 (1956), pp 70-74

[12] N. Grenier, J.-P. Vila and P.Villedieu. An accurate low-mach scheme for a compressible two-uid model applied to free-surface ows. J. Computational Phys., 252:119, 2013.